Effects of ion bombardment on the nucleation and growth of diamond films

X. Jiang,* W. J. Zhang, and C.-P. Klages
Fraunhofer-Institut für Schicht- und Oberflächentechnik, Bienroder Weg 54 E, D-38108 Braunschweig, Germany
(Received 3 November 1997; revised manuscript received 30 March 1998)

The influence of ion bombardment on the nucleation and growth of diamond films by microwave plasma chemical vapor deposition (CVD) has been investigated. The following findings were obtained. (i) Modification of surface diffusion by a substrate bias voltage was demonstrated by the measurement of the first-nearest-neighbor distances. The satisfactory agreement of the nucleation rate with a kinetic model describing the formation of active sites, germs, and nuclei was computer-simulated using crystal-size-distribution data under consideration of a linear growth mechanism. (ii) A dependence of growth direction of diamond grains upon the orientation of ion bombardment was observed using an atomic force microscopic analysis. (iii) Using a combination of scanning electron microscopy and transmission electron microscopy, slight misorientations of crystallites, homoepitaxially grown on (001) diamond faces parallel to the substrate, were found and analyzed. The findings confirm the role of ion impact in diamond CVD and help to understand the basic mechanism responsible for the crystal orientation in heteroepitaxial diamond films prepared using bias-enhanced nucleation. A detailed study of H^+ ion etching selectivity was performed in order to obtain insight into the basic mechanism of the observed effects. [S0163-1829(98)04135-6]

I. INTRODUCTION

It is well known[1] that the kinetic energy of vapor particles strongly influences the physical vapor deposition (PVD) of thin films. Physical processes on or near the growth surface can be modified by the bombardment by energetic particles. As the extent of bombardment increases, the sticking probability of the vapor atoms on the surface increases due to the formation of active sites; the mobility and the diffusion of adatoms/adsorbed species will be enhanced. With a high enough kinetic energy (e.g., >30 eV), surface penetration (subplantation) of the particles and even backsputtering of the deposited atoms can occur. These surface processes influence the morphology, the crystallinity, and the properties of the deposited films. For plasma-assisted chemical vapor deposition (PACVD), ion bombardment also plays an important role. A typical example is the deposition of amorphous hydrocarbon films.[2,3] With increasing substrate bias voltage, the film structure changes from polymerlike through diamondlike to graphitelike due to the increased extent of ion bombardment. Modification of diamond CVD by ion bombardment has also been observed since 1990.[4–6] Previous investigations revealed different effects of the negative substrate bias voltage. In the early studies,[4,5] a negative influence of ion bombardment on diamond growth, namely the amorphitization of the diamond surface to an amorphous phase, was observed. On the other hand, enhanced diamond nucleation by application of ion bombardment was first reported by Yugo *et al.*[6] This bias-enhanced nucleation has then attracted considerable interest after the heteroepitaxy of diamond on silicon carbide and silicon substrates was achieved using this method.[7,8] The mechanism of this enhanced nucleation has been studied by different groups and very different models have been reported. Yugo *et al.*[9] and Gerber *et al.*[10,11] suggested a shallow ion implantation model, in which the sp^3-bonded carbon clusters, formed by ion implantation, serve as nucleation precursors. Stoner *et al.*,[12,13] on the other hand, suggested that the change in plasma chemistry, such as the increase in atomic hydrogen concentration due to the substrate biasing and the formation of a carbide surface layer, should play the decisive role. Jiang *et al.*[14,15] found that the overall temporal evolution of nucleation density agrees well with a surface kinetic model involving immobile active nucleation sites, germs, and nuclei established by Tomellini *et al.*[16] They have further suggested that ion bombardment can increase the density of surface defects (point defects, steps, and sp^3-bonded carbon clusters), which can serve as the nucleation sites and also enhance surface diffusion and sticking probability of carbon on silicon. The enhancement of surface diffusion of carbon species was identified in an investigation of the first-nearest-neighbor distance distributions.[14]

A complete explanation of the mechanism of bias-enhanced epitaxial nucleation is still a theme being studied intensively. Nevertheless, more experimental results have been reported to show the decisive role of ion bombardment.[17,18]

Recently it was observed[19,20] that (001)-textured diamond films can be prepared by application of a suitable negative substrate bias potential during diamond growth, resulting in the selective growth of certain growth surfaces. This growth selectivity was attributed to the suppression of the growth of the non-[001] grains due to the electron emission under bias[19] and reactive ion etching due to ion bombardment.[20] Furthermore, it was shown that the orientation of a diamond layer grown under ion bombardment depends not only on the orientation of the underlying crystals (epitaxy), but also on the direction of the ion flow towards the substrates. Secondary nucleation of [001] oriented crystallites on non-(001) crystallographic planes of diamond crystals has been observed.[21]

While the substrate biasing during diamond CVD has made successes for the heteroepitaxial nucleation and oriented growth, the investigation of the effects of ion bom-

 © 1998 The American Physical Society

TABLE I. Preparation conditions of the specimens.

Process	H_2 concentration (vol.%)	CH_4 concentration (vol.%)	Gas pressure (mbar)	Substrate temp. (°C)	Bias voltage (V)	Power (W)
Plasma etching[a]	100	0	25	850	−150	900
Nucleation[a]	98	2	20	850	−150	900
Bias-assisted growth[b]	99.6	0.4	25–30	780	−150–+150	900
Bias-assisted H^+ etching	100	0	30	780	−150	1000

[a]Plasma etching for cleaning the substrates lasts 20 min; the nucleation times for different samples are 0, 2.5, 5, 7.5, 10, 12, 15 min. respectively.

[b]⟨100⟩-textured, ⟨111⟩-textured, and randomly oriented films were used as substrates.

bardment is not only of great scientific importance but also of significant technological value for further improving the textured growth of diamond films. The purpose of this paper is to study the effects and mechanism of ion bombardment–enhanced nucleation and growth during microwave plasma CVD of diamond. Due to the fact that diamond nucleation and growth take place on surfaces of largely different energies [6 J/cm^2 for diamond, 1.5 J/cm^2 for the silicon (111) plane][22,23] and conductivities, the growth modes are therefore different. In this paper the effect of ion bombardment on nucleation will be discussed first and the experimental results on the effect on growth will be presented. Finally, the results on the H^+ ion etching effect will be shown.

II. EXPERIMENT

The nucleation and growth of diamond films were performed in a microwave plasma CVD system. Heterogeneous nucleation of diamond crystallites was achieved *in situ* on 2-in. *n*-type (001) silicon wafers by applying a negative bias potential to the substrate.

The wafers were chemically cleaned with acetone in an ultrasonic bath for 10 min and then loaded into a stainless-steel ASTeX reactor. After evacuating the chamber to a pressure of about 10^{-3} mbar, the substrate was etched *in situ* in a hydrogen microwave plasma for 20 min to remove the native surface oxide layer. Diamond nuclei were then formed in a 2% methane-in-hydrogen microwave plasma. To study the nucleation kinetics, samples were prepared under various negative substrate bias voltages and different nucleation times. The deposition parameters are given in Table I.

To investigate the effects of ion bombardment during the growth stage, differently oriented diamond films biased at various voltages were used as substrates and the growth phenomena were observed. Experiments using only the hydrogen as a reactant gas were also performed to distinguish between the ion etching mechanism and a textured growth mechanism. The substrates were dc biased at −150 V relative to the vacuum chamber, which was electrically grounded. The experimental details for this process are also given in Table I.

III. EFFECTS OF ION BOMBARDMENT DURING NUCLEATION STAGE

A. General description of the diamond nucleation

The formation mechanism of diamond crystallites under the effect of a substrate bias voltage is presently still under controversial discussion.[15] This is due to the difficulties of distinguishing the aspects of plasma–chemical vapor deposition (the presence of a reactive gas species of thermal energy at the substrate) and physical vapor deposition (PVD, hyperthermal ionic species bombarding the substrate). As already mentioned in the Introduction, different models have been presented.

Nucleation is the first step of a film growth. Generally, the nucleation of a new phase requires the formation of a nucleus exceeding a critical size and becoming thermodynamically stable. According to the kinetic theory, the nucleation may be described by the following sequence: (a) vapor species arrive on the substrate surface (atoms, molecules, and/or radicals) and are adsorbed; (b) the species diffuse over the substrate surface and part of the adatoms desorbs from the surface into the vacuum; (c) the adatoms combine and form clusters due to fluctuations of the local species concentration; (d) nuclei grow by capturing the adatoms or by direct impingement of the atoms from the vapor phase. The critical size of the nuclei depends on the total free enthalpy of formation related to the free energies of the surfaces of nuclei and substrate. Because of the strong bonding and an energetic advantage, the nuclei form preferentially on surface defects, such as steps, dislocations, or surface impurities. Such surface defects were often called ''active'' sites for film nucleation.

The diamond nucleation in a CVD process via a substrate bias voltage should also follow the recognized sequence. In comparison with this sequence, the models mentioned in the Introduction have only considered the possible key factors of the processes critically influencing the nucleation. For example, the subplantation of hyperthermal ions leads to the formation of sp^3-bonded amorphous carbon. This foreign phase (with respect to the diamond phase), in addition to a possible variation of plasma chemistry, may reduce the formation enthalpy of diamond nuclei. The surface kinetics enhanced by the ion bombardment can accelerate the nucleation. In the following section we would like to present results demonstrating the important role of substrate biasing for diamond nucleation and the effects of the bias-induced ion bombardment. The results support the above-described nucleation sequence.

B. The decisive role of ion bombardment for the bias-enhanced diamond nucleation

Heteroepitaxial nucleation of diamond on Si or SiC is to date limited to microwave plasma CVD (Refs. 7, 8, 24, and

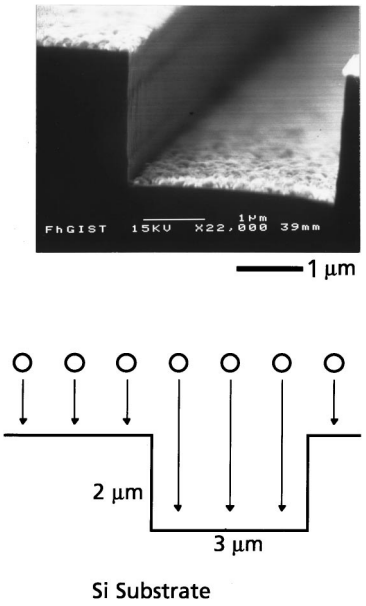

FIG. 1. Selective growth of diamond crystals on a grooved silicon wafer containing both faces perpendicular and parallel to the substrate. The different nucleation densities on the faces confirm the decisive role of ion bombardment for the diamond nucleation.

25) and hot-filament CVD processes[26,27] owing to the success of nucleation by biasing the substrate without any other *ex situ* pretreatment. Without substrate pretreatment, epitaxial CVD diamond has only been reproducibly grown on diamond and on *c*-BN, which is lattice matched and chemically compatible to diamond.[28]

To identify the effect of substrate biasing, different experiments have been carried out using the grooved (001) oriented silicon substrate obtained using reactive ion etching[17,29] as well as SiO_2-masked silicon substrates.[30,31] Using reactive ion etching, a grooved (001) oriented silicon substrate, containing surfaces both parallel and perpendicular to the silicon wafer, was prepared (Fig. 1). When a negative electrical potential was applied to the substrate, the positively charged ions in the plasma were accelerated towards the wafer. The surfaces that are parallel to the wafer will be bombarded while the perpendicular surfaces will not (please see the schematic diagram of Fig. 1). As a result, diamond was only nucleated on surfaces parallel to the wafer, while the perpendicular surfaces were completely ''clean.'' The decisive contribution of the ion bombardment to the diamond nucleation was therefore clearly demonstrated.

The nucleation of diamond on silicon depends sensitively on the substrate bias potential.[32] A critical bias voltage exists, beyond which the energy barrier for the formation of stable nuclei can be overcome. The attraction of positively charged energetic ions due to the negative bias increases the bombardment of the substrate surface, which has two effects: Creation of surface defects of the substrate, which will serve as active nucleation sites, and enhancement of the surface diffusion of adatoms (see Sec. III D).

C. Agreement of the bias-enhanced nucleation with kinetic modeling

In Ref. 14 the dependencies of island density and size distribution on the deposition time were analyzed by means

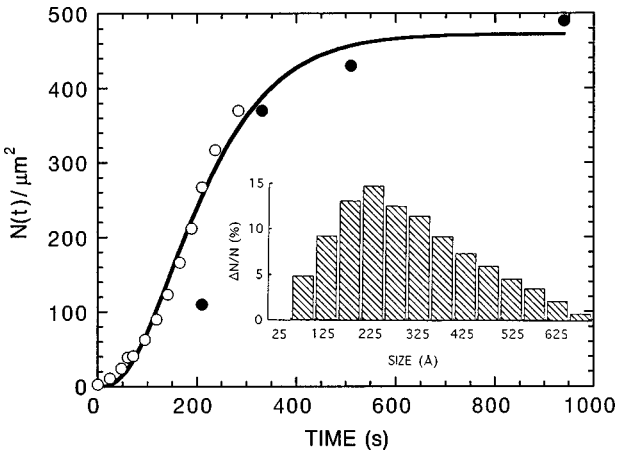

FIG. 2. Nucleation density (islands/μm^2) vs deposition time. In the abscissa an induction time of 6.5 min is subtracted. The curve is obtained by computer modeling using *three-step kinetic* models proposed by Tomellini and Polini. The open and full circles in the plots represent data calculated from crystal size distribution (inset) and obtained by direct particle counting, respectively.

of scanning electron microscopy. By a model established by Tomellini *et al.*,[16] a kinetic approach to the nucleation data was made providing a definite framework on a molecular scale. The proposed model predicts the time evolution of active sites, germs, and nuclei of the substrate surface and includes the capture of germs and active sites at the borders of the growing diamond phase. By solving three differential equations, written in terms of the surface densities of active sites, germs, and nuclei, the nucleation density $N(t)$ of well-separated islands on solid surfaces can be obtained. One problem appearing in this approach is that only five experimental points were compared with the simulation results leading to a relatively large uncertainty. To solve this problem, simulations were performed using experimentally measured size distribution data (see the inset of Fig. 2). The time dependence of nucleation density was calculated by establishing a relationship between the particle radius distribution function and the nucleation rate through the knowledge of the nucleus growth law.[33]

Figure 2 shows the nucleation density as a function of the nucleation time compared with simulated results by a three-step kinetic model. The data directly measured by particle counting are also shown for comparison (full circles in the plots). The three steps were modified by Polini and Tomellini[33] by introducing an extra step for the generation of nucleation sites, i.e., the kinetic scheme is now

$$R \rightarrow N^{+} \leftrightarrow m \rightarrow N, \tag{1}$$

where R, N^{+}, m, and N are densities of the surface centers that can be transformed into a nucleation site, the nucleation sites, the unstable clusters, and the stable nuclei (=nucleation density). The modification is reasonable because only unscratched silicon wafers were used as substrate and the nucleation sites were formed during the bias-enhanced nucleation stage.

The nucleation density N (islands/cm^2) is plotted in Fig. 2 as a function of nucleation time t, which is counted from the induction time t_{ind}. The t_{ind} is generally defined as a time when the aggregates formed initially have grown to a diam-

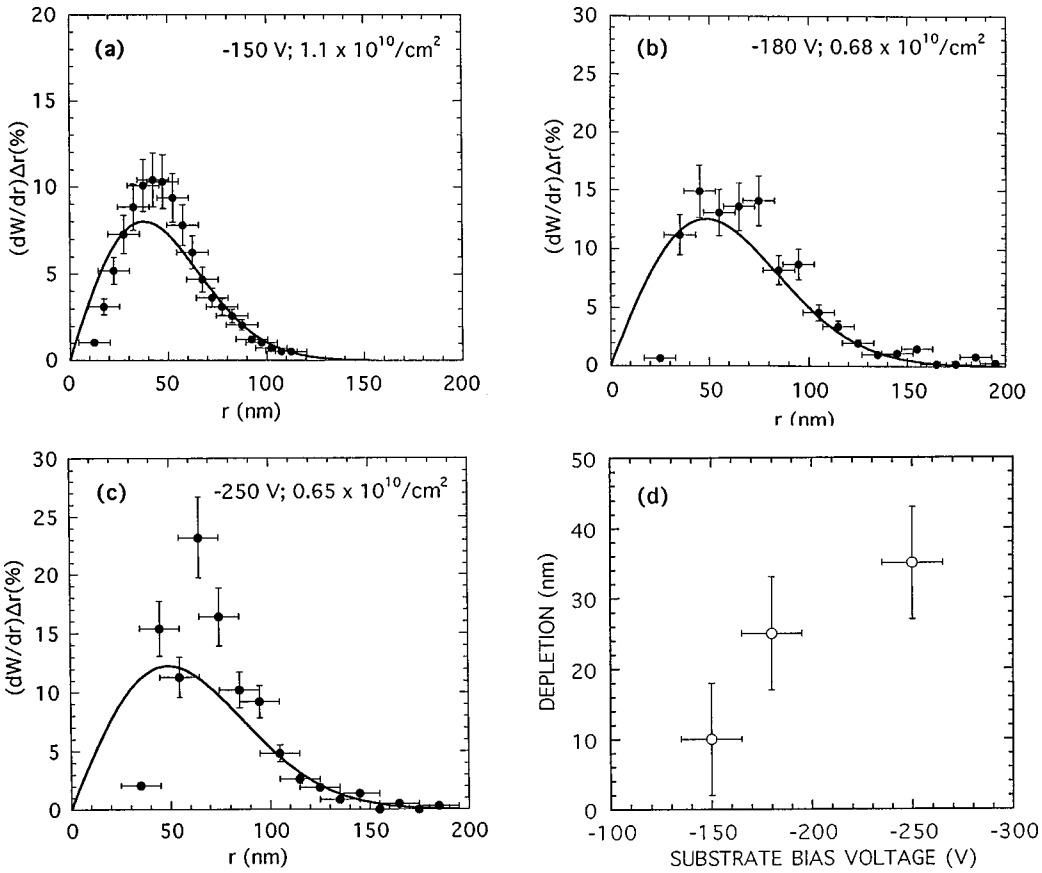

FIG. 3. Comparisons of measured nearest-neighbor distance distributions and the distributions predicted from a random nucleation model for samples prepared under different substrate bias voltages. (a) $V_b = -150$ V; (b) $V_b = -180$ V; (c) $V_b = -250$ V; (d) depletion distance vs V_b.

eter that is detectable in the electron microscope. As the resolution of modern scanning electron microscopy is in the order of a nanometer, which can be reached by the nuclei within one minute after nucleation, the t_{ind} can also be understood as the period for production of the nucleation sites. According to the results obtained by AFM and RHEED, the induction time in this study is about 6.5 min. From Fig. 2 it is evident that, once the nucleation begins, the nucleation density increases rapidly to 4.3×10^{10} cm^{-2} within 8.5 min. The main part of the substrate surface is then covered by the nuclei and the increase of the density, i.e., the nucleation rate is lowered with increasing coverage. It was found that, under the conditions applied in this study, the whole substrate surface is covered by the diamond nuclei to form a continuous film after about 25 min deposition.

From Fig. 2 it can be noticed that the nucleation kinetics derived from the size distribution function (open circles in the plot, deposition time=12 min) is close to the result directly measured by particle counting at different times (full circles) and the diamond nucleation agrees very well with kinetics of the established surface process.

D. First nearest-neighbor distance distribution: A measure of surface diffusion

The morphology and the position distribution of nuclei on a biased silicon (001) surface were also investigated by SEM and AFM. It was noticed that the established nuclei tend to stay more away from each other than expected from a random distribution and that a depletion zone around each nucleus was observed. From these results, a model on the growth kinetics as determined by the adatom diffusion effect was suggested: The formation of depletion zones around the islands is due to the surface diffusion leading to a drop of the concentration of the adsorbed precursors in the immediate neighborhood of the islands. The islands can be considered as sinks for the surface precursors.

If the suggested surface diffusion is truly responsible for the observed depletion and furthermore for the diamond nucleation, one should expect that the dimension of the depletion will depend on the substrate bias potential, because the mobility of adatoms is expected to increase due to the increasing energy of bombarding ions. To study this effect, new samples were prepared under various bias voltages and the nearest-neighbor distance distributions were investigated.

When the nuclei are dispersed randomly on the support the theoretical distributions of first nearest neighbors $W(r)$ can be derived from the calculations established (solid lines in Fig. 3).[14] The nearest neighbor is defined such that there is no crystallite within a distance r from a crystallite taken as an origin, and that at a distance between r and $r+dr$ one notes the presence of a crystallite that is the first nearest neighbor,

$$dW_{\mathrm{random}}(r,dr) = 2\pi r\rho\ \exp(-\rho\pi r^2)dr = W_{\mathrm{random}}(r)dr, \tag{2}$$

where ρ is the number density of crystallites dispersed randomly. From the SEM images, we can measure the distributions,

$$W_{\text{measured}}(r)=\rho(r,dr)/N, \tag{3}$$

where $\rho(r,dr)$ is the number of islands with nearest-neighbor distance between r and $r+dr$ and N is the total number of islands counted. Such measurements have been performed by Schmeisser *et al.*[34,35] for the evaporated Au/NaCl system and by Yang *et al.*[36] for the evaporated Ge/GaAs system.

Figure 3 compares the measured distributions $W_{\text{measured}}(r)$ with calculated distributions of the first nearest neighbors corresponding to a random distribution $W_{\text{random}}(r)$ for diamond nuclei deposited under -150, -180, and -250 V, respectively. The nucleation densities of different samples were kept at a similar range and were $1.1\times10^{10}/\text{cm}^2$, $0.68\times10^{10}/\text{cm}^2$, and $0.65\times10^{10}/\text{cm}^2$, respectively.

All the measured distributions in Figs. 3(a)–3(c) are shifted to larger distances in comparison to the random distributions $W_{\text{random}}(r)$ and depletion zones of different sizes around each cluster were observed. The depletion zone of the nuclei increases from 12 nm for $V_b=-150$ V to 35 nm for $V_b=-250$ V [Fig. 3(d)].

These results imply that the diamond nucleation is strongly influenced by the existing nuclei—an effective ''repulsive interaction'' among the clusters exists and the clusters tend to separate. Two effects should be considered to interpret the results. First, the lattice strain field in the vicinity of an island that leads to a repulsive ''force'' for the formation of another nucleus due to an increase in the energy barrier for the formation of an island. Ascarelli, Cappelli, and Pinzari[37] studied the origin of a nucleation density depletion around each diamond nucleus found in Ref. 14 and came to the conclusion that the depletion is related to a deformation zone induced by the diamond-silicon lattice misfit. The second possible interpretation is the above-mentioned surface diffusion of the adsorbed precursors. Due to a decrease of the precursor concentration to zero on the border of one island, the nucleation frequency drops down to zero. The fact that the depletion is a function of substrate bias voltage [Fig. 3(d)] confirms the contribution of surface diffusion to the depletion. Due to the bias-induced ion bombardment, the mobility and the diffusion of adsorbed species on the substrate surface will be increased and the spatial extension of the surface diffusion–caused depletion zone decrease will be increased. The depletion zone size should correspond to the minimum distance from a nucleus where the precursor concentration is influenced by the existing nucleus. The role of the surface diffusion of the species for CVD diamond growth has recently been investigated by Flanklach *et al.*[38]

To summarize the results obtained for the nucleation stage, the decisive role of ion bombardment for the diamond nucleation and the surface diffusion of the species forming diamond has been confirmed. The diamond nucleation rate agrees with the calculated value by a kinetic model of surface processes. Based on these results, the nucleation sequence can be given as follows.

(i) *Formation of nucleation sites.* The nucleation sites can be considered as sites having high local surface energy, such as defects and surface impurities. According to the classical thermodynamic theory, the critical size of the nuclei, which determines the nucleation frequency, depends on the surface energies of substrate and deposit. The nucleation would be easier on the high-energy sites to minimize the energy barrier and to stabilize the system. Due to an increased ion bombardment, a shallow subplantation of carbon ions can occur if the ion energy is large enough (>20 eV).[10] The implanted atoms occupy sites in the host lattice resulting in localized stress and increase the surface energy. One important factor of applying a substrate bias for accelerating the nucleation is the interruption of the Si-H bonding (abstraction of the adsorbed hydrogen). This leads to an increase of the sticking coefficient of hydrocarbon radicals to form high-energy nucleation sites.[39]

(ii) *Formation of carbon clusters due to the enhanced surface diffusion.* Applying a negative substrate potential will increase the bombardment by positively charged energetic ions and thus increase the mobility of surface precursors and hence the probability of forming clusters. The enlargement of the first-nearest-neighbor distance provides strong evidence for the adatom diffusion.

(iii) *Formation of stable diamond nuclei.* Once the clusters reach the critical size (corresponding to the energy barrier of diamond nucleation, the critical dimension depends on the experimental conditions and is still unknown), the growth stage begins. The attraction of the positively charged hydrocarbon species, which leads to a carbon supersaturation at the substrate surface, and the increasing generation of atomic hydrogen may make a contribution to the nucleation rate.

After the formation of nuclei, the substrate bias should be turned off to avoid the formation of defects and amorphitization of the nuclei leading to a secondary nucleation onto an established island. This renucleation negatively influences the epitaxial film growth due to the interruption of the Van der Drift growth. Recently, however, a new effect of ion bombardment was found that a proper substrate bias voltage could affect the film orientation and could be helpful for a [001]-oriented diamond growth. The kinetic energy of the arriving particles seems to be critical for the observed effect.[19,20] To utilize the potential of ion bombardment for oriented film growth, a detailed investigation of the effects of ion bombardment in the growth stage was performed.

IV. EFFECTS OF ION BOMBARDMENT IN THE GROWTH STAGE

A. [001]-textured growth on randomly oriented and [111]-textured diamond film substrates

Diamond films have been grown onto large-grained, partially [001]-oriented diamond films at biased voltages from -150 to $+150$ V. The process parameters are shown in Table I. The electrical potential was kept at the substrate throughout the experiments so that, in case of a negative potential, the substrate surface would be continuously bombarded by energetic ions. According to the axis-symmetric experimental geometry, the ions flow in a direction perpendicular to the substrate as confirmed by the selective nucleation via biasing the substrate.[17]

Figure 4 shows the SEM images of the diamond films prepared under different bias voltages. The gas pressure was 25 mbar. The films that were prepared with positive bias

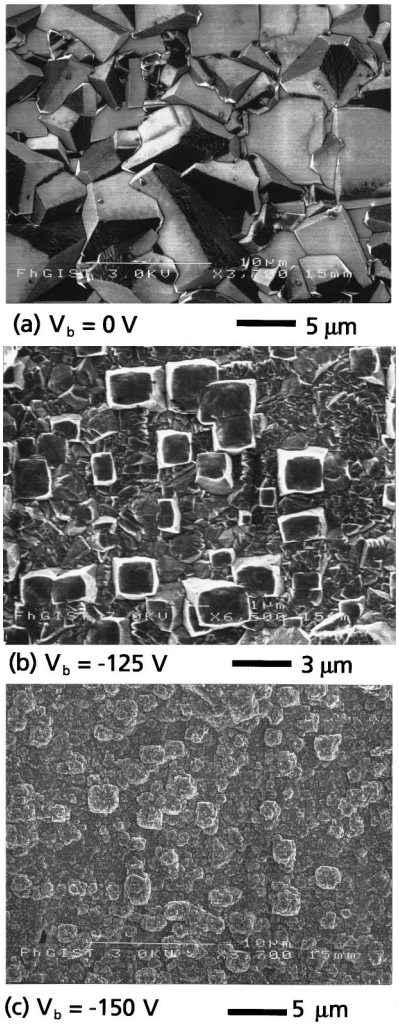

FIG. 4. SEM morphologies of the films prepared under different substrate bias voltages. (a) $V_b = 0$ V; (b) $V_b = -125$ V; (c) $V_b = -150$ V.

voltage do not provide any change of the surface morphology in comparison with the films prepared without bias [Fig. 4(a)]. A morphology variation occurred first at a negative voltage of -100 V. Figure 4(b) shows a SEM image of a film after 20 h growth under bias-induced ion bombardment (substrate bias voltage $V_b = -125$ V). A significant variation of the film morphology was achieved: The top film was covered by diamond crystals of [001] orientation. The epitaxial [001] grains protrude from the film surface and the non-[001] top grains keep lower positions. With a bias voltage of -150 V, the surface becomes fine crystalline as shown in Fig. 4(c), although the square contour of the original (001) facets is still visible.

Further experiments showed that the bias-induced textured growth depends mainly on the parameters that influence the particle energy (e.g., substrate bias voltage and process pressure) and occurs within a very small parameter window. If one works at a higher pressure, the ion energy will decrease due to the increasing probability of ion-neutral collisions. Correspondingly, the bias voltage for the textured growth should increase. Figure 5 shows SEM surface images of a 10-μm-thick diamond film substrate prepared without bias (a) and a film after 20 h growth under bias-induced ion

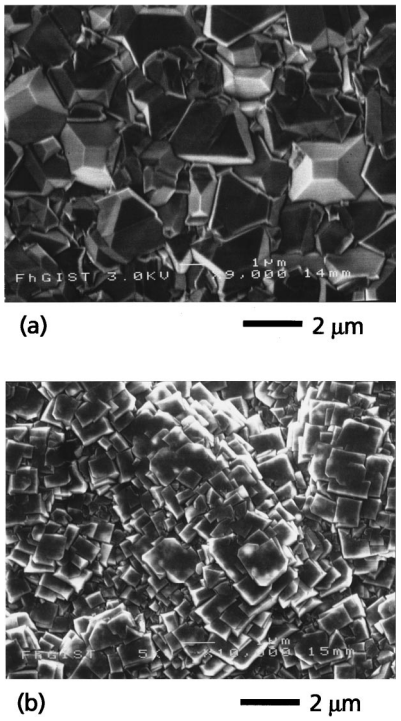

FIG. 5. Scanning electron micrographs of (a) a randomly oriented diamond film (used as a substrate); (b) the top layer grown under bias voltage of $V_b = -150$ V for 20 h.

bombardment (b). The gas pressure was increased to 30 mbar and the bias voltage must be increased to a value of $V_b = -150$ V in order to obtain optimal film morphology. A significant variation of film morphology was achieved: the top layer of the film changes from a randomly oriented film to completely [001] textured. The [001]-oriented crystallites shown in Fig. 5(b) have a lateral size of about 0.5 μm, smaller than the underlying crystallites shown in Fig. 5(a). Domains containing parallel-oriented crystallites are clearly seen in Fig. 5(b).

To study the development of the orientation and the orientation relationship between crystallites of the top layer and the underlying grains, diamond films were grown, under bias condition, onto a specially prepared ⟨111⟩ textured polycrystalline diamond film. Figure 6 shows the SEM surface images of films prior to and after bias-assisted deposition of different deposition times. Prior to bias-assisted deposition, the triangular (111) face of the large diamond grain is essentially smooth except some triangular growth hillocks with edges along the ⟨110⟩ direction [Fig. 6(a)]. After growth for 3 h [Fig. 6(b)], the hillocks became steep and a few small triangular islands were formed on the substrate (111) surface. These top islands have their (111) crystal facets parallel to the (111) substrate surface and their ⟨110⟩ edges aligned parallel to each other and to the corresponding substrate ⟨110⟩ directions. The (111) face of the large underlying crystal is clearly rougher than that before bias-assisted deposition. As the growth time increases, the amount of the top islands increases and a few grains of the [001] direction are formed among these triangular islands after bias-assisted deposition for 5 h, as indicated by the arrows in Fig. 6(c).

A surprising phenomenon was observed after bias-assisted deposition for 10 h. As shown in Fig. 6(d), the sub-

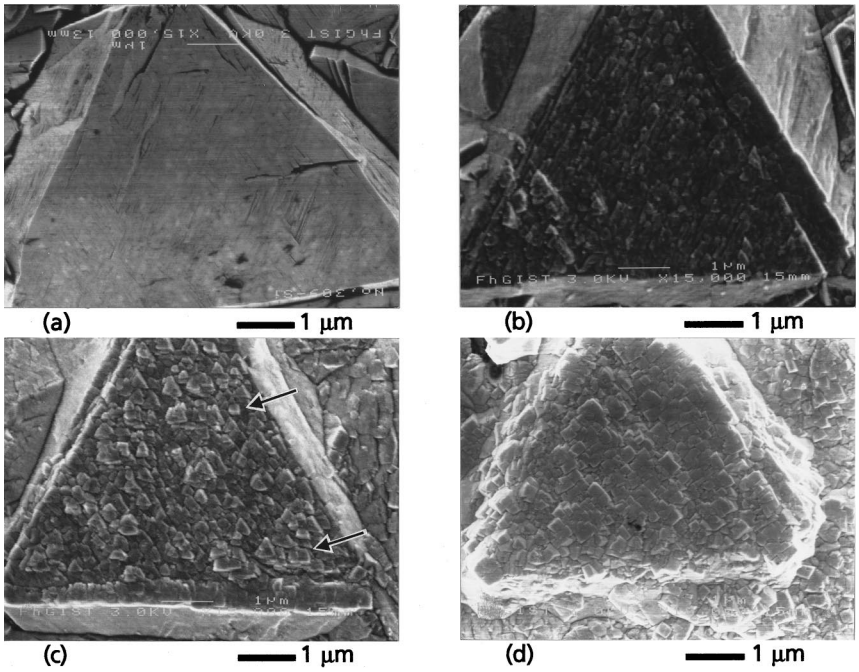

FIG. 6. Scanning electron microscopic images of the (111) facets for different deposition time under −150 V bias voltage. (a) Prior to bias-assisted deposition; (b), (c), (d) after bias-assisted deposition for 3, 5, and 10 h, respectively.

strate (111) face is now mainly covered by a top layer of [001]-textured crystallites, i.e., their (001) facets are parallel to the substrate (111) facet. These top [001] crystallites are even in-plane oriented with their ⟨110⟩ edges aligned parallel to each other and parallel to one of the ⟨110⟩ axes of the underlying crystals. The observed phenomenon is obviously a result of crystal renucleation producing crystallites with a certain orientation relationship to the substrate, but are not in an identical crystal direction. The growth orientation of the top crystallites is clearly determined not only by the substrate orientation ($\langle 110\rangle_{\text{top crystallites}} \| \langle 110\rangle_{\text{underlying crystal}}$) but also by the ion flux direction, i.e., the [001] axis is parallel to the ion flux. If only the effect of ion bombardment were considered, an ⟨001⟩-textured top layer would grow, i.e., the in-plane orientation of the top layer should be random. In contrast, if only the effect of the substrate crystal direction were considered, the homoepitaxial growth should continue.

To further reveal the nature of the observed [001]-textured growth, investigation of bias-assisted growth was done by SEM on faces that are tilted with respect to the silicon substrate. Figure 7 shows SEM images of two large crystals after 6 h bias-assisted growth. Schematic representations of the large crystals are also shown in the figure illustrating the facets of the crystals before bias-assisted deposition. The surface of the [001]-oriented crystal (a) consists of four {111} facets and the surface of the [110]-oriented crystal (b) consists of two {111} and two {100} facets exposed to the gas phase during deposition. In this case the faces are clearly not oriented parallel to the substrate. On the large crystals, small crystallites of sizes of 0.5 μm were grown. Interestingly, it was seen that even on the faces whose normal is not parallel to the substrate normal, parallel oriented small crystals were grown. These [001]-oriented crystallites are marked by small arrows.

To study the relationship between the grain orientation and the ion flux direction, atomic force microscopy (AFM) was performed. Figure 8(a) shows an AFM image of a diamond top layer formed on a (001) face of a large diamond grain of a 10-μm-thick film. The (001) face in Fig. 8(a) is tilted by 10° around the [110] axis and by −3° around the [110] axis, respectively, with respect to the silicon substrate as measured by the quantitative picture analysis. The top layer after deposition consists of completely [001] (also in-plane) oriented crystallites with a lateral size of about 0.5 μm. The [001] crystallites are not in identical orientation with the underlying large crystal. The tilt angle distributions of the [001]-textured crystallites were measured along the [110] and [110] axes and are shown in Fig. 8(b). The tilt angle distributions obtained are similar to those observed in films epitaxially grown on (001) silicon. Tilt misorientations follow the statistical Gaussan distribution with a full width at half maximum (FWHM) of 8°. Oriented crystallites grown with in-plan misorientation to the diamond substrate have been observed previously[20] and will be discussed in detail in the following section. As expected, the maximum of the orientation distributions shifted to 10° about the [110] axis and −3° about the [110] axis. Because the crystal tilting of the analyzed (001) face of the underlying crystal was corrected for the tilt measurements, giving the (001) face in Fig. 8(a) of an exact horizontal orientation, the measured distribution shifts in Fig. 8(b) resulted due to the parallel orientation relationship between the [001] axes of the small crystallites and the ion flux direction. From this quantitative confirmation, the following conclusions can be made: even for the {100} crystal faces, if they are not in identical orientation with the substrate (silicon), the on-top homoepitaxial growth will be interrupted and a renucleation of the diamond growth occurs. The [001] axis of the grown diamond grains is always along the ion flow direction, perpendicular to the substrate and independent of the crystal orientation of underlying crystals.

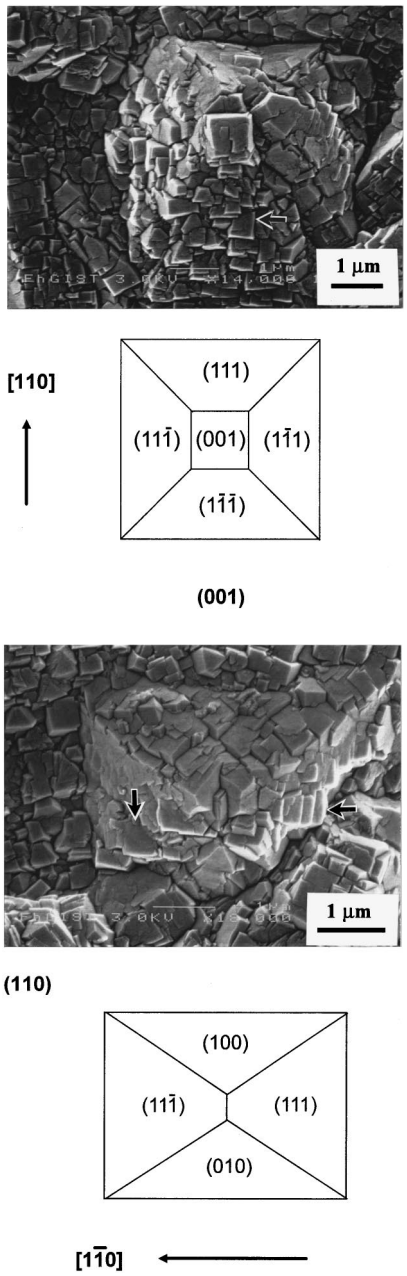

FIG. 7. SEM images of two large crystals after 10 h bias-assisted growth together with schematic representations.

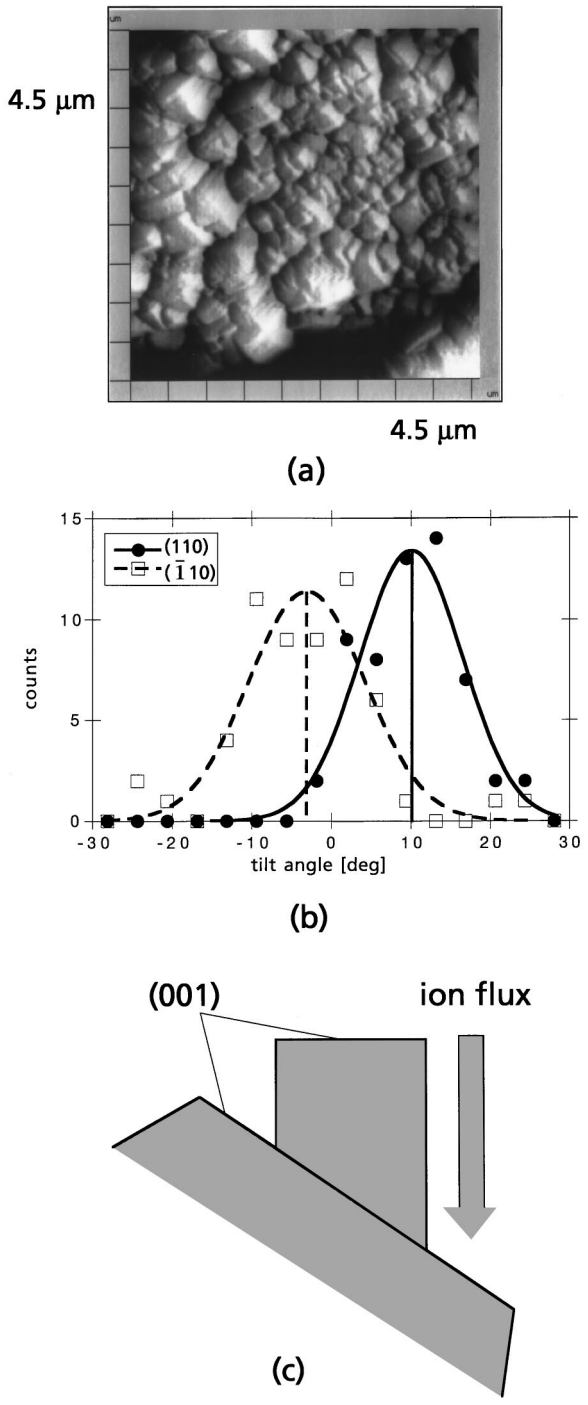

FIG. 8. Atomic force microscopic topography of the tilt (001) face after bias-assisted deposition (a) and tilt angle distributions along [110] and [1$\bar{1}$0] axes measured by a quantitative picture analysis (b), confirming the parallel orientation relationship between the top layer crystals and the ion flux as schematically shown in (c).

It is also interesting to note that, as already shown in Fig. 6(d), the newly grown diamond crystals shown in Fig. 7 are aligned parallel with each other and have one of their ⟨110⟩ axes parallel to one of the ⟨110⟩ axes of the large substrate crystal. This occurs when the ⟨110⟩ axes are lying in the (001) plane and demonstrates the influence of the substrate crystal on the orientation of on-top grown crystallites.

It is a complicated task to interpret the effects of ion bombardment on diamond film growth. The observed [001]-textured film growth is, obviously, not a result of ''evolutionary selection,'' which ascribes the film texture to the different growth rates for {111} and {100} faces, dominantly governed by the substrate temperature and the hydrocarbon gas concentration used for deposition. Under the used experimental conditions of the film growth, the {100} surfaces grow more slowly than other surfaces if a negative substrate bias is not applied. A possible mechanism for the growth of (100) faceted crystals is the crystal twinning. It is known that multiple twinning may lead to (100) faceted crystals even on (111) substrates.[40] However, no multiple crystal twinning was identifiable from our studies of the temporal evolution of crystal morphology of the (111) diamond face under bias condition.[21] From the cross-sectional SEM observations, it was found that for the deposition on the (111) diamond sur-

face there exists a sharp transition of crystal orientation from [111] to [001]. The ion-flow-direction dependent film growth can therefore only be a result of the ion impact, a physical factor in diamond CVD.

It was found for PVD (physical vapor deposition) thin-film deposition assisted by ion bombardment that the degree of orientation order was a function of the intensity of the ion flux, i.e., ion/atom flux ratio, and the incident angle of the ion flow.[41] The orientation of the films was due to the sputtering yield, which is dependent on the relative orientation of the film crystal to the ion flux. To explain the phenomenon that a (001) textured layer was deposited on a diamond film of random crystal direction, the role of the substrate bias voltage must be considered. The diamond growth is generally a combined process of deposition and reetching taking place concurrently. A film grows if the deposition rate is larger than the reetching rate. During the deposition process of diamond film by CVD, atomic H and H^+ ions in the plasma are known to cause etching, H^+ ions etching much faster than atomic H. For the deposition under bias condition, H^+ ions are accelerated towards the substrate, and the reactive ion etching caused by H^+ ions is expected to play a dominant role. The etching yield of H^+ is probably dependent on the relative orientations between the ion flow and the growing grain. It can therefore be argued that the selection mechanism for grain orientation is due to the difference in etching yields between grains that are oriented (in our case the [001] textured) and those that are not. The different etching yields on different faces, which can be as high as a factor of 5 in some PVD processes, combined with renucleation, leads to a film growth for aligned grains, and hence to an overall orientation order. The selective etching by H^+ ions and its effects on the oriented growth of diamond films were studied by using pure hydrogen as reactant gas and are discussed in a separate section.

The ion impact damages the surface of the substrate and introduces a large amount of active sites for secondary nucleation (renucleation) interrupting the homoepitaxial growth. This leads to a decrease in the efficient free path (diffusion length) of the adsorbed surface precursors and furthermore the average lateral size of the top [001]-textured crystallites decreased to only about 0.5 μm, much smaller than that of the underlying substrate crystals.

From the threefold symmetry of the (111) diamond face, it is expected that a [001]-textured growth should involve crystallites of three possible in-plane orientations. It was, however, observed in Fig. 6(d) that all the crystallites are parallel to only one of the three ⟨110⟩ edges. This could be a result of the slight crystal tilt that is visible in the figure. The threefold symmetry was destroyed by tilting the crystal. In fact, the parallel oriented growth of the crystallites occurred only on a part of the (111) faces that are tilted to the substrate. On the (111) faces with no tilting, three groups of crystallites were grown with their ⟨110⟩ edges parallel to the three ⟨110⟩ edges of the underlying crystals.[21]

B. Ion bombardment–induced misorientation on (001) heteroepitaxial growth

If the underlying diamond crystals have their [001] axes parallel to the ion flow direction, the homoepitaxial process

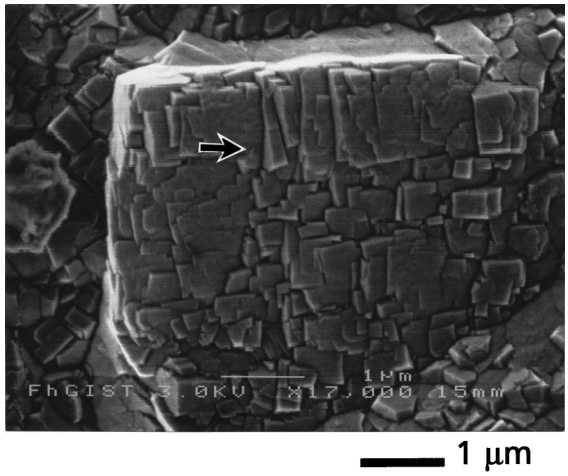

FIG. 9. Morphology of the top layer grown under bias condition on a large (001) oriented crystal.

on the (001) top faces continues. Then (001) oriented top layers were grown, consisting of crystallites with sizes of the order of 0.5×0.5 μm^2. Figure 9 is a SEM image showing the small parallel-oriented crystallites with the crystal edges aligned to one another on a 4×4 μm^2 (001) square underlying face. It is interesting to note that, in contrast to a conventional homoepitaxial growth (without biasing the substrate), the on-top grown crystallites were observed to have a small misorientation to the underlying single crystal. The arrows in Fig. 9 labeled several such crystallites. The image shown in Fig. 9 is very similar to the film morphology obtained from a heteroepitaxial film grown directly on the (001) silicon substrate by the bias-enhanced nucleation: The film has an identical overall orientation to the (001) silicon, however with a statistical misorientation of a couple of degrees to the substrates.[8]

To confirm the ion bombardment–induced misorientation, transmission electron microscopy (TEM) was employed. The TEM image of the top layer is shown in Fig. 10 together with the selective-area electron diffraction pattern. The misorientation was clearly demonstrated by the diffraction. Detailed information about the TEM investigation will be described elsewhere.[42]

The observed slight misorientation may provide us with a valuable hint about the origin of the previously observed misorientation of the heteroepitaxial diamond films on silicon and on other kinds of substrates. This misorientation has often been attributed to the lattice mismatch between diamond and the substrate used.[26,43] After the observation that diamond on silicon has a 3-to-2 multiple lattice match, it was claimed that the misorientation should be due to the defects formed at the interface.[17,44] From Fig. 9 it is clear that, even for a homoepitaxial diamond growth that has the perfect lattice match, a misorientation of the on-top grown crystallites occurs, if the substrate is biased. High-resolution transmission electron microscopy (HREM) interfacial investigations revealed[45] that, in the region of diamond nucleation, poor crystallinity of the interface was often observed between the silicon substrate and the diamond crystallites with crystal misorientation to the substrate. These results support strongly the explanation of the defect formation within the crystals at the growth interface. Further detailed investiga-

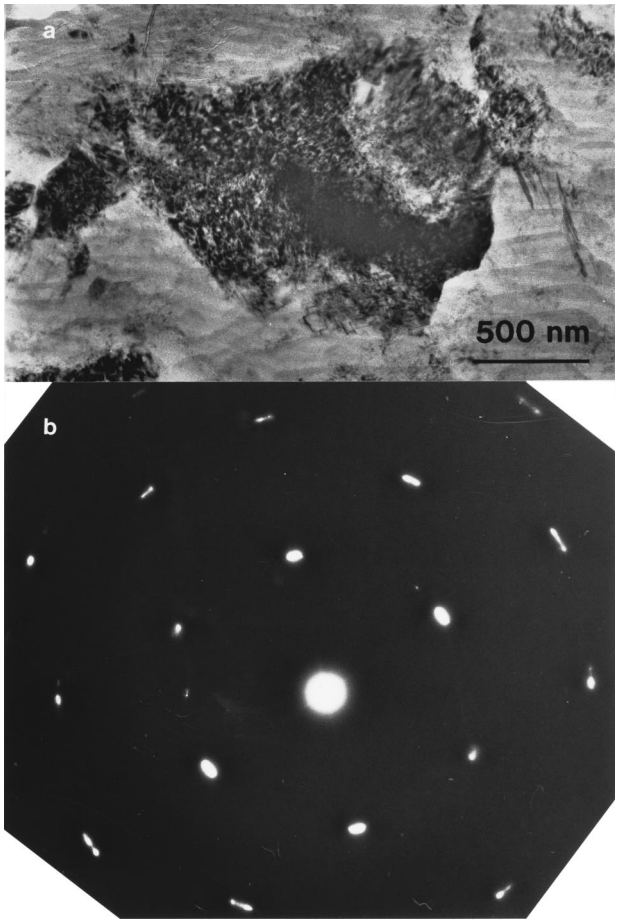

FIG. 10. Transmission electron microscopic image (a) and the electron diffraction pattern (b) of the bias-assisted top layer.

tion of the interface between the diamond substrate crystal and the top layer grown by bias-assisted deposition is of importance to confirm this prediction.

C. Investigation of the selective etching of H^+ ions as the origin of the oriented bias-assisted film growth and its use for textured film growth

As is demonstrated in Sec. III A, the [001]-textured top layer can be prepared on differently oriented diamond films by applying a negative substrate bias potential during diamond growth. The selective etching caused by H^+ ions during deposition is supposed to play a decisive role. Due to the facts that the growth process is a combined process of deposition and etching and the presence of methane in the gas phase, the hypothesis, however, cannot be confirmed experimentally. It is difficult to distinguish the contributions of the selective H^+ etching and [001] preferential growth.

To prove the reported selection mechanism due to the orientation-dependent etching yields, the selective etching effect of H^+ ions on the differently oriented diamond faces using pure hydrogen as reactant gas was investigated. Furthermore, this selective etching was used for the preparation of oriented diamond films.

The experiment was divided into three steps: (i) [001]-oriented diamond films were deposited on mirror-polished (001) silicon wafers after bias-enhanced nucleation; (ii) the samples deposited in the first step were etched *in situ* in hydrogen plasma by setting an electrical potential at -150 V to the substrate relative to the reactant chamber; (iii) the samples were deposited once again under the deposition conditions as in step (i). The process parameters for the bias-assisted plasma etching in step (ii) are given in Table I.

The surface morphologies and the cross-sections of the film were observed by SEM before and after the bias-assisted hydrogen etching process [step (ii)]. The average etching rate of the films was about 0.05 μm/h, which was calculated by the thickness difference of the film cross sections. Figure 11(a) shows the SEM surface image before etching. Large [001] grains and some grains with undefined crystal direction were observed. The average size of the (001) faces of the large grains is about 1μm. After 20 h bias-assisted H^+ etching, the surface morphology changes strongly, as shown in Fig. 11(b). The [001]-oriented crystals become more dominant in the image. The (001) faces are rougher. The average size of the (001) facets of the large [001] grains increases up to nearly 2 μm.

The results demonstrate the effect of the selective etching of diamond grains by H^+ ions to the morphology of the films. The contribution of the etching by atomic hydrogen to the selectivity can be ruled out because it causes only an improvement in the film quality but not the film orientation.[46,47]

When hydrogen ions in the plasma are accelerated towards the substrate during the bias-assisted etching, the energy and the amount of H^+ ions bombarding the substrate increase in comparison with that without bias. Due to the lower atom density of the {100} face relative to the {111} face, more H^+ ions can channel through the lattice of oriented (001) faces with their normal along the [001] direction. In contrast, the {111} faces have the highest atom density and the impact probability of hydrogen ions with atoms on the {111} plane should be high. The etching efficiency of H^+ ions is therefore lower for (001) faces than for {111} faces. To explain the phenomenon that the (001) faces that are parallel with the substrate become larger after H^+ ions etching, a redeposition should be taken into account during the H^+ ions etching process. The H^+ ions will etch off the carbon atoms from the diamond face forming hydrocarbon species (such as CH, CH_2, and CH_3) that could be neutral or charged positively. The hydrocarbon clusters charged positively will be accelerated towards the substrate due to the negative bias potential and then neutralized by capturing electrons from the substrate, so the carbon partial pressure near the substrate surface is higher than the etching process without substrate bias. The redeposition process can occur during the etching procedure. The etching efficiency of H^+ ions on the non-[001] oriented grains is higher than that on [001] grains with their [001] normal parallel to the ion flux. Hence, the (001) faces will survive and become larger due to the local chemical transport reaction while the non-[001] grains will be etched off.

It was found experimentally in our laboratory that the renucleation of diamond crystallites and the etching rate of hydrogen ions due to the substrate biasing depend critically on the bias voltage applied. The variation of the ion energy enables therefore a control of not only the textured but also the epitaxial diamond growth. As a logical consequence, the selective etching effect is utilized to improve the epitaxial growth of [001]-oriented films.

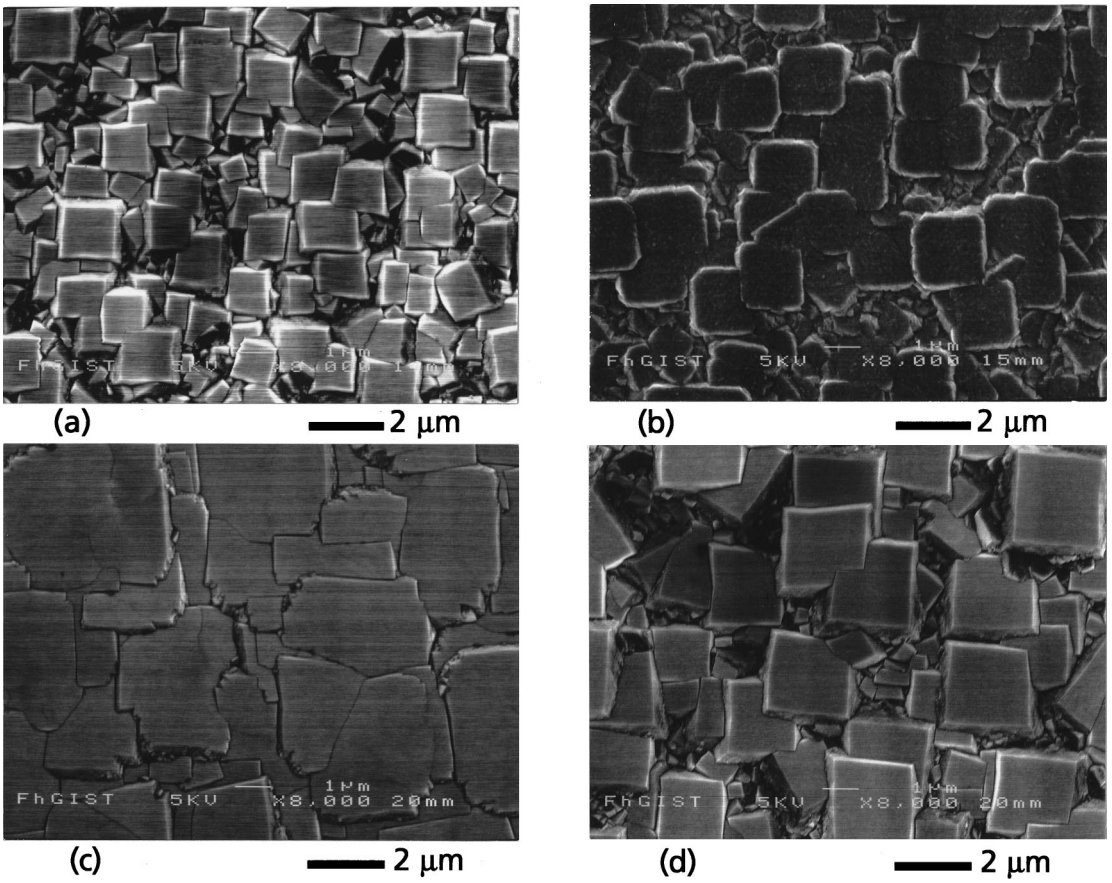

FIG. 11. SEM morphologies of a diamond film before (a) and after (b) a bias-assisted hydrogen etching for 20 h. (c) shows the SEM surface image of a diamond film deposited by a three-step process: 20 h deposition with bias-enhanced nucleation, 20 h H^+ ions etching and 20 h deposition. (d) is from the sample deposited without bias-assisted H^+ ion etching but for the same deposition time (40 h) and under the identical deposition conditions.

Figure 11(c) shows an SEM image of a diamond film deposited by a three-step process: 20 h deposition with bias-enhanced nucleation, 20 h H^+ ion etching, and 20 h deposition. It can be seen that the film consists of completely [001]-oriented grains. The surface of the film is smooth and clear. For the sample deposited without bias-assisted H^+ ion etching but for the same deposition time (40 h) and under the identical deposition conditions as for the sample in Fig. 11(c), the surface morphology differs considerably [Fig. 11(d)]. Non-[001] grains still exist among the large [001] grains.

Raman investigations showed a minor change of the crystal quality of the on-top grown films. A too-long etching process (e.g., $>$60 h) can, however, lead to a fine crystalline structure. The grain boundaries and the sp^2 component of the film increase.

The selectivity of H^+ ion etching on differently oriented diamond grains and its assistance in improving the orientation accuracy of diamond film are clearly shown, which is different from the methods reported in previous papers for preparing textured films.[48,49] For previously reported methods the oriented diamond films were prepared by a two-step process that varies the ratio of growth rate $V_{(001)}/V_{(111)}$ by changing the substrate temperature and gas composition in the plasma. The diamond grains of non-[001] direction were covered up by [001] grains, and the orientation grade of films increases with the film thickness. In the etching process, the orientation grade of the film was increased by etching the grains with the other direction away. In other words, this effect is possibly helpful for obtaining an [001]-oriented diamond film with small film thickness.

V. SUMMARIES AND CONCLUSIONS

The effects of ion bombardment on both stages of nucleation and growth in microwave plasma assisted diamond CVD have been investigated. It has been shown that the increased ion bombardment modifies the nucleation and growth behavior of CVD diamond films enormously. By biasing the substrate, oriented diamond nuclei can be generated with very high density up to $5\times10^{10}/\mathrm{cm}^2$. During the deposition stage, ion bombardment leads to a renucleation of diamond on randomly oriented crystals and a selectivity of the diamond growth. Both effects observed in this work can be effectively employed for improving epitaxial and textured diamond film growth. For example, a texture of the diamond film is achievable right at the beginning of the deposition by the application of a proper bias voltage to the substrates.

Disadvantages of the ion bombardment were also observed. These include the formation of amorphous carbon phase and the creation of crystal defects. It was demonstrated that even on the single crystalline diamond, polycrystalline top layers with crystal misorientation will be obtained when substrate biasing was used. This identifies, at least, the con-

tribution of ion bombardment induced crystal defects to the observed misorientation. To improve the heteroepitaxy of diamond films, these disadvantages of ion bombardment must be overcome.

ACKNOWLEDGMENTS

The authors thank M. Paul, K. Schiffmann (FhG-IST, Braunschweig), and D. Wittorf (KFA-IFF, Jülich) for their assistance in film preparation and film characterizations with AFM and TEM, respectively. We acknowledge R. Polini and M. Tomellini (University of Roma) for their help and discussions about the computer simulations, and C. S. Lee (City University of Hong Kong) for a critical reading the manuscript. One of the authors (W.J.Z.) thanks the Federal Ministry of Education, Science, Research and Technology (BMBF) for financial support.

*Electronic address: jiang@ist.fhg.de

[1] K. Reichelt and X. Jiang, Thin Solid Films **191**, 91 (1990).
[2] X. Jiang, Phys. Rev. B **43**, 2372 (1991).
[3] X. Jiang, J. W. Zou, K. Reichelt, and P. Grünberg, J. Appl. Phys. **66**, 4729 (1989).
[4] S. Yugo, T. Kimura, and T. Muto, Vacuum **41**, 1364 (1992).
[5] G.-H. M. Ma, Y. H. Lee, and J. T. Glass, J. Mater. Res. **5**, 2367 (1990).
[6] S. Yugo, T. Kanai, T. Kimura, and T. Muto, Appl. Phys. Lett. **58**, 1036 (1991).
[7] B. Stoner and J. T. Glas, Appl. Phys. Lett. **60**, 698 (1992).
[8] X. Jiang and C.-P. Klages, Diamond Relat. Mater. **2**, 1112 (1993); X. Jiang, C.-P. Klages, R. Zachai, M. Hartweg, and H.-J. Füßer, Appl. Phys. Lett. **62**, 3438 (1993).
[9] S. Yugo, T. Kimura, and T. Kanai, Diamond Relat. Mater. **2**, 328 (1993).
[10] J. Gerber, S. Sattel, K. Jung, H. Ehrhardt, and J. Robertson, Diamond Relat. Mater. **4**, 559 (1995).
[11] S. Sattel, J. Gerber, and H. Ehrhardt, Phys. Status Solidi A **154**, 141 (1996).
[12] B. R. Stoner, G. H. Ma, S. D. Wolter, W. Zhu, Y.-C. Wang, R. F. Davis, and J. T. Glass, Diamond Relat. Mater. **2**, 142 (1993).
[13] B. R. Stoner, S. R. Sahaida, J. P. Bade, P. Southworth, and P. J. Ellis, J. Mater. Res. **8**, 1334 (1993).
[14] X. Jiang, K. Schiffmann, and C.-P. Klages, Phys. Rev. B **50**, 8402 (1994).
[15] X. Jiang and C.-P. Klages, Phys. Status Solidi A **154**, 175 (1996).
[16] M. Tomellini, R. Polini, and V. Sessa, J. Appl. Phys. **70**, 7573 (1991).
[17] X. Jiang, M. Paul, C.-P. Klages, and C. L. Jia, in *Diamond Materials IV*, edited by K. V. Ravi and J. P. Dismukes (The Electrochemical Society, Pennington, NJ, 1995), Vol. 95-4, p. 50.
[18] S. McGinnis, M. Kelly, and S. B. Hagström, Appl. Phys. Lett. **66**, 3117 (1995).
[19] J. S. Lee, K. S. Liu, and I. N. Lin, Appl. Phys. Lett. **67**, 1555 (1995).
[20] X. Jiang, W. J. Zhang, M. Paul, and C.-P. Klages, Appl. Phys. Lett. **68**, 1927 (1996).
[21] W. J. Zhang and X. Jiang, Appl. Phys. Lett. **68**, 2195 (1996).
[22] *The Properties of Diamond*, edited by J. E. Field (Academic, London, 1979).
[23] K. Ishibashi and S. Furukawa, Jpn. J. Appl. Phys., Part 1 **24**, 912 (1985).
[24] R. Hessmer, M. Schreck, S. Geier, B. Rauschenbach, and B. Stritzker, in *Advances in New Diamond Science and Technology*, edited by S. Saito, N. Fujimori, O. Fukunaga, M. Kamo, K. Kobashi, and M. Yoshikawa (MYU, Tokyo, 1994), p. 235.
[25] H. Maeda, M. Irie, T. Hino, K. Kusakabe, and S. Morooka, J. Mater. Res. **10**, 158 (1995).
[26] J. Yang, Z. Lin, L.-X. Wang, S. Jin, and Z. Zhang, Appl. Phys. Lett. **65**, 3203 (1994).
[27] F. Stubhan, M. Ferguson, H.-J. Füßer, and R. J. Behm, Appl. Phys. Lett. **66**, 1900 (1995).
[28] S. Koizumi, T. Murakami, T. Inuzuka, and K. Suzuki, Appl. Phys. Lett. **57**, 563 (1990).
[29] A. Flöter, G. Schaarschmidt, B. Mainz, S. Laufer, S. Deutschmann, and H.-J. Hinneberg, Diamond. Relat. Mater. **4**, 930 (1995).
[30] X. Jiang, E. Boettger, M. Paul, and C.-P. Klages, Appl. Phys. Lett. **65**, 1519 (1994).
[31] S. Yogo, K. Semoto, K. Hoshina, and T. Kimura, in *Advances in New Diamond Science and Technology*, edited by S. Saito, N. Fujimori, O. Fukunaga, M. Kamo, K. Kobashi, and M. Yoshikawa (MYU, Tokyo, 1994), p. 175.
[32] X. Jiang, C.-P. Klages, R. Zachai, M. Hartweg, and H.-J. Füßer, Diamond Relat. Mater. **2**, 407 (1993).
[33] R. Polini and M. Tomelini, Diamond Relat. Mater. **4**, 1311 (1995).
[34] H. Schmeisser and M. Harsdorff, Philos. Mag. **27**, 739 (1973).
[35] H. Schmeisser, Thin Solid Films **22**, 83 (1974).
[36] Y.-N. Yang, Y. S. Luo, and J. H. Weaver, Phys. Rev. B **46**, 15 387 (1992).
[37] P. Ascarelli, E. Cappelli, and F. Pinzari, Appl. Phys. Lett. **70**, 1697 (1997).
[38] M. Flanklach, S. Skokov, and B. Weiner, in *Diamond Materials IV*, edited by K. V. Ravi and J. P. Dismukes (The Electrochemical Society, Pennington, NJ, 1995), Vol. 95-4, p. 1.
[39] Z. D. Lin (private communication).
[40] C. Wild, R. Kohl, N. Herres, W. Müller-Sebert, and P. Koidl, Diamond Relat. Mater. **3**, 373 (1994).
[41] L. S. Yu, J. M. E. Harper, J. J. Cuomo, and D. A. Smith, Appl. Phys. Lett. **47**, 932 (1985).
[42] D. Wittorf *et al.* (unpublished).
[43] W. Zhu, X. H. Wang, B. R. Stoner, G.-H. M. Ma, H. S. Kong, M. W. H. Braun, and J. T. Glass, Phys. Rev. B **47**, 6529 (1993).
[44] X. Jiang and C. L. Jia, Appl. Phys. Lett. **67**, 1197 (1995).
[45] C. L. Jia *et al.* (unpublished).
[46] B. Cline, W. Howard, H. Wang, K. E. Spear, and M. Frenklach, J. Appl. Phys. **72**, 5926 (1991).
[47] D. S. Olsen, M. A. Kelly, S. Kapoor, and S. B. Hangstrom, J. Mater. Res. **9**, 1546 (1994).
[48] C. Wild, P. Koidl, W. Müller-Sebert, H. Walcher, R. Kohl, N. Herres, R. Locher, R. Samlenski, and R. Bree, Diamond Relat. Mater. **2**, 158 (1993).
[49] CH. Kawarada, T. Suesada, and H. Nagasawa, Appl. Phys. Lett. **66**, 583 (1995).